

Sources of error in tetrapolar impedance measurements on biomaterials and other ionic conductors

Sverre Grimnes^{1,2} and Ørjan G Martinsen^{1,3}

¹ Department of Physics, University of Oslo, PO Box 1048 Blindern, NO-0316 Oslo, Norway

² Department of Clinical and Biomedical Engineering, Rikshospitalet, Oslo, Norway

E-mail: ogm@fys.uio.no

Received 3 July 2006, in final form 24 September 2006

Published 15 December 2006

Online at stacks.iop.org/JPhysD/40/9

Abstract

Tetrapolar electrode systems are commonly used for impedance measurements on biomaterials and other ionic conductors. They are generally believed to be immune to the influence from electrode polarization impedance and little can be found in the literature about possible pitfalls or sources of error when using tetrapolar electrode systems. In this paper we show that electrode polarization impedance can indeed influence the measurements and that also other phenomena such as negative sensitivity regions, separate current paths and common-mode signals may seriously spoil the measured data.

1. Introduction

Tetrapolar electrode systems (four-electrode systems) are commonly used for electric impedance measurements in a number of research areas from bioimpedance measurements on single cells to geological measurements on the lithosphere. Due to its ability to largely reduce the influence of electrode polarization impedance, this electrode system has been very popular but little has been written about possible sources of error introduced by the tetrapolar system. Hence, some authors do not discuss the electrode configuration [1, 2].

It is nevertheless a fact that tetrapolar systems are more vulnerable to errors than monopolar or bipolar systems [3, 4]. It is usually stated or assumed that tetrapolar systems are not prone to errors from electrode polarization impedance [5, 6]. In this paper, however, we will show that this is not necessarily true. We will also discuss some other common problems introduced by the system. The sensitivity field of tetrapolar systems has, for instance, zones of negative sensitivity, which may introduce large errors when measuring on heterogeneous materials [7] and the signal pick-up (PU) electrodes may have a common mode voltage (CMV) which precludes the use of common Kramers–Kronig control [8, 9].

³ Author to whom any correspondence should be addressed.

2. The sensitivity field of a tetrapolar system

When measuring the impedance of a material with a tetrapolar electrode system, it is intuitively understood that not all small sub-volumes in the material contribute equally to the measured impedance. Volumes between and close to the electrodes contribute more than volumes far away from the electrodes. Hence, a careful choice of electrode size and placement will enable the user to focus the measurements on the desired part of the material. It is a common misunderstanding that if the electrodes are placed in a linear fashion, with the voltage PU electrodes between the current carrying (CC) electrodes, only the volume between the voltage PU electrodes is measured. Not only is this wrong, but there will also be zones of negative sensitivity between the voltage PU electrodes and the CC electrodes. Negative sensitivity means that if the impedivity is increased in these zones, lower total impedance will be measured. This is contra-intuitive and the phenomenon is not much discussed in the literature. Using finite element modelling, a plot of the sensitivity field of a measuring set-up on a given material can easily be provided, and this method provides a very valuable tool for experimental design.

The sensitivity of a small volume dV within the measured biomaterial is a measure of how much this volume contributes to the total measured impedance [10], provided that the electrical properties (e.g. resistivity) are uniform throughout

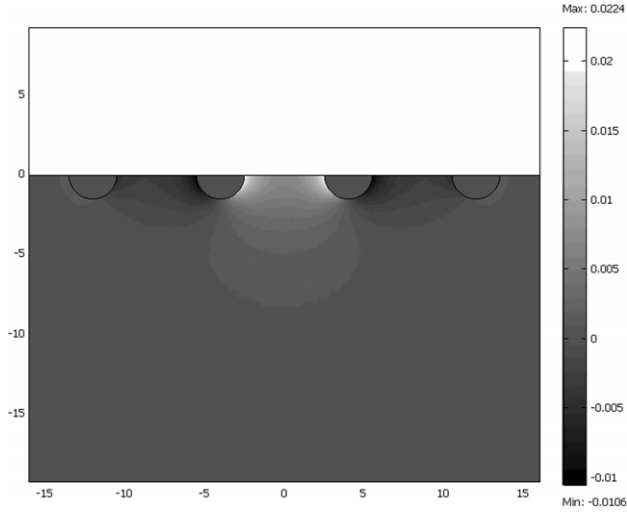


Figure 1. Sensitivity distribution of a tetrapolar electrode system.

the material. If, in this case, the resistivity varies within the material, the local resistivity must be multiplied with the sensitivity to give a measure of the volume's contribution to the total measured resistance.

If we look at a simple example of a direct current resistance measurement with a four-electrode system, the sensitivity will be computed in the following way:

1. Imagine that you inject a current I between the two CC electrodes and compute the current density \mathbf{J}_1 in each small volume element in the material as a result of this current.
2. Imagine that you instead inject the same current between the voltage PU electrodes and again compute the resulting current density \mathbf{J}_2 in each small volume element.
3. The vector dot product between \mathbf{J}_1 and \mathbf{J}_2 in each volume element, divided by the current squared, is now the sensitivity of the volume element, and if we multiply with the resistivity ρ in the volume, we will directly get this volume's contribution to the total measured resistance R .

Hence the sensitivity S and the total measured resistance R will be

$$S = \frac{\mathbf{J}_1 \cdot \mathbf{J}_2}{I^2} \quad \text{and} \quad R = \int_V \frac{\rho \mathbf{J}_1 \cdot \mathbf{J}_2}{I^2} dv.$$

A positive value for the sensitivity means that if the resistivity of this volume element is increased, a higher total resistance will be measured. The higher the value for the sensitivity, the greater the influence on the measured resistance. A negative value for the sensitivity, on the other hand, means that increased resistivity in that volume gives a lower total measured resistance. A four-electrode system will typically have small volumes with negative sensitivity between the CC and voltage PU electrodes. This is clearly shown in figure 1, where the sensitivity distribution of a tetrapolar system is calculated. The finite element calculations on four half-cylinders submerged into the material have been done in the commercial software package Comsol Multiphysics.

These equations also demonstrate the reciprocal nature of the tetrapolar system (or any other electrode system where this

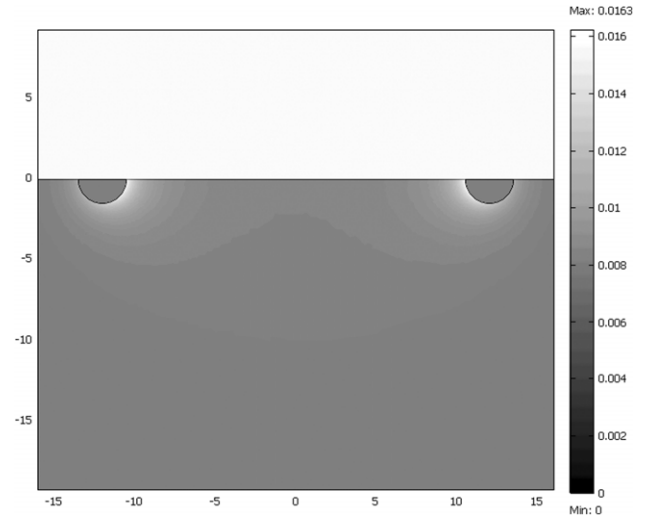


Figure 2. Sensitivity distribution of a dipolar electrode system.

theory applies); under linear conditions the CC electrodes and voltage PU electrodes can be interchanged without any change in measured values.

Sensitivity calculations can be utilized equally well for two- three- or four-electrode systems. In each case you must identify the two electrodes used for driving an electrical current through the material and the two electrodes used for measuring the potential drop in the material.

In the case of a two-electrode system, these two electrode pairs are the same, and the sensitivity in a given volume will hence be the square of the current density divided by the square of the total injected current.

In figure 2 the sensitivity distribution in a dipolar system is shown with only positive values.

More research should be carried out on how, for example, negative sensitivity influences the measurements and what sort of measurement errors this phenomenon could potentially introduce.

3. Current paths and electrode placement

Measuring a positive phase angle on materials with resistive/capacitive properties is commonly taken as a sign of measurement error. In some cases, as discussed in section 6, the positive phase angle can be due to self-inductance in the medium, but in many cases there are other reasons for this phenomenon.

3.1. Equivalent circuits and network analysis

Figure 3(a) shows a simplified network to illustrate possible characteristic properties of a tetrapolar measuring system used, for example, on biological tissue. The resistor R has been chosen without parallel capacitance to make it easier to follow the phase characteristics. This is a single path series network, and with ideal components there is no phase shift between the externally measured current i and voltage v . The measured voltage will lag the measured current with a capacitor in parallel with R (negative phase angle). The

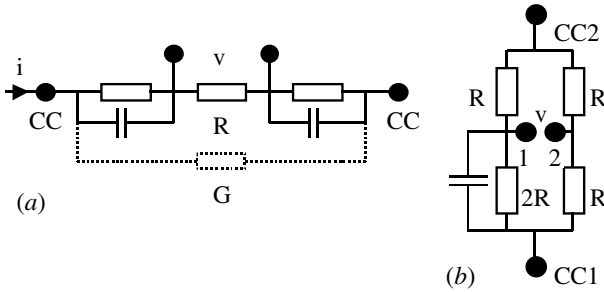


Figure 3. Simple four-terminal, two-port networks. (a) Single series current path, with second path stippled. (b) Bridge.

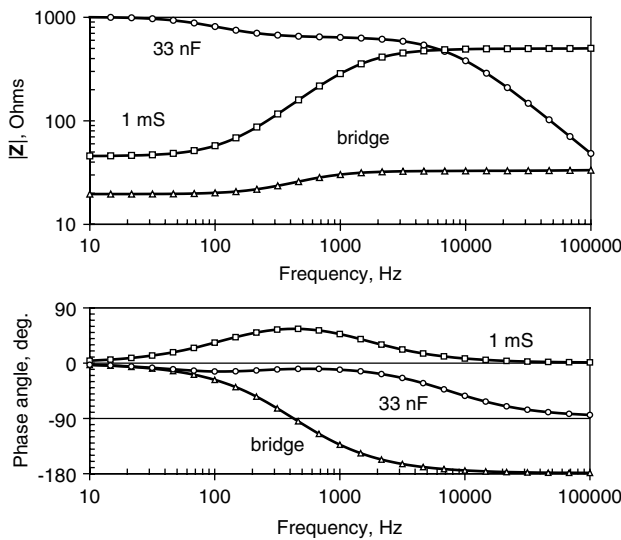


Figure 4. Bode plot for the networks of figure 3. Component values: $R = 1 \text{ k}\Omega$, parallel combination $10 \text{ k}\Omega$ and $0.1 \mu\text{F}$, $G = 1 \text{ mS}$ or $C = 33 \text{ nF}$. Bridge: $R = 100 \Omega$, $C = 2.3 \mu\text{F}$.

transfer impedance [11] is

$$\mathbf{Z} = \frac{v' + jv''}{i}$$

In order to obtain a positive phase characteristic, a second path in parallel (G) can be introduced as indicated in figure 3(a). The current i is then divided into two paths, and the value of the current through R is no longer known from external measurements. If G has a much higher conductance than the series path admittance and i is constant, $|v|$ will clearly increase with frequency because of the two capacitors. The capacitive current through R (and therefore v) will lead the current i . We will also study the case where the parallel conductance G has been replaced by a pure capacitance.

Figure 4 shows the Bode plot of these cases. The network with a conductance G has positive phase transfer impedance where the maximum possible phase shift is $+90^\circ$. With increasing frequency the phase is positive and the transfer impedance is increasing. The totally different result with a parallel capacitor shows how important are the properties of the second current path.

Hence, in materials where there is more than one current path in parallel, one may measure a positive phase angle even if there are no inductive properties present. In tissue this

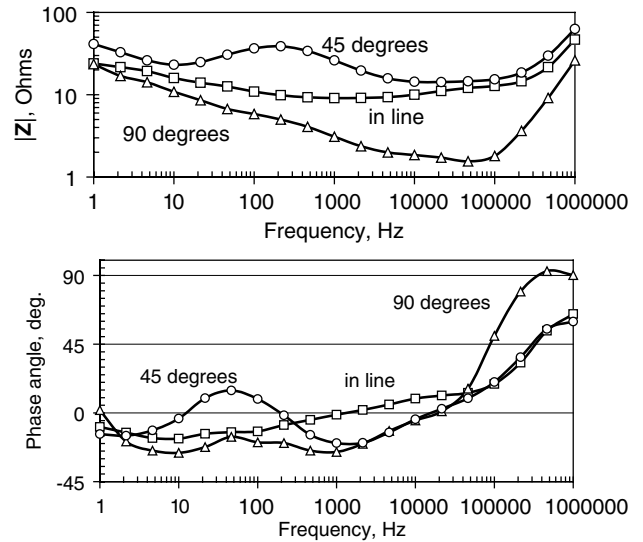


Figure 5. Transfer impedance found with skin surface PU electrodes oriented parallel, oblique 45° and perpendicular to the presumed current density direction.

is almost always the case; tissue is inhomogeneous and the current density will be distributed according to the impedivities in the tissue. The skin in particular is highly stratified with low and high admittivity layers.

It is possible to extend the positive phase shift to 180° by introducing a bridge circuit, such as in figures 3(b) and 4. With the values as shown it is clear that at low frequencies v is in phase with the current, meaning that the voltage at terminal 1 is positive when the current i (and voltage at CC2) is positive. As the frequency is increased, the voltage at terminal 1 will start to lag terminal 2, and the transfer impedance will have a negative phase, but with increasing magnitude. At higher frequencies the magnitude of the impedance of the $2R$ - C combination will be lower than R , and the phase shift will extend up to -180° . At high frequencies v actually is again in phase with i , but for the external measurement the low impedance of the capacitor has had the effect of swapping the terminals, turning the phase by 180° . As pointed out by Kuo [11], a bridge is a non-minimum phase network.

3.2. Human tissue data

A simple experiment was conducted by placing two dry AgCl-covered disc electrodes 10 mm in diameter and with a fixed centre distance of 15 mm as voltage PU electrodes on the forearm of a volunteer. Two commercial wet gel electrodes with a skin wetted area of 3 cm^2 were used as CC electrodes and placed on the hand and upper arm, respectively. One measurement was taken with the PU electrodes oriented along presumed current density lines, one at a 45° angle and one perpendicular to that direction. Measurements were performed with a Solartron 1260 + 1294 system in the frequency range 1 Hz–1 MHz. Controlled voltage mode was used, with a level of 1 V rms. With the CC-electrodes used the current was in the range $10 \mu\text{A}$ rms (LF) to 3 mA (HF).

The results in figure 5 show a strong positive phase transfer impedance. The transfer impedance is in the range 2–60 Ω . The positive phase crossover frequency is around 1 kHz for

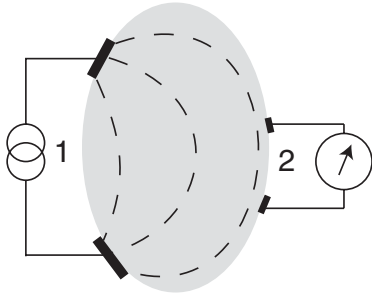


Figure 6. Tissue-electrode model.

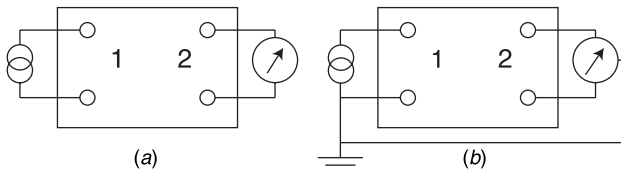


Figure 7. Black boxes, four-terminal, two-port versions. (a) Ideal version. (b) An often found practical version.

longitudinal electrode direction and 20 kHz for the oblique and perpendicular cases. For the oblique electrode orientation a second frequency range with positive phase occurs around 40 Hz. The positive phase values are accompanied by increasing impedance magnitudes.

Hence, this simple experiment shows that positive phase transfer impedance is explainable from parallel current paths in purely resistive-capacitive systems. A positive phase characteristic should therefore not necessarily be interpreted as inductive properties of tissue. Instead it illustrates the very complex sensitivity situation found with tetrapolar electrode systems. The results are in agreement with Gersing *et al* [12], who focused upon the influence of the polarization capacitance of the CC electrodes giving different current density phase angles for different current path lengths. The earlier belief that the tetrapolar method is independent of electrode polarization impedance is then no longer always valid. Our models show, however, that tissue electrical properties and electrode positions also may be the reason for the positive phase angle found.

We have shown increasing impedance magnitudes with frequency accompanied by either positive or negative phase characteristic. It remains to be analysed whether non-minimum phase networks as shown are compatible with the Kramers-Kronig transforms [13].

4. Common-mode signals

Problems with common-mode signals (CMS) are deeply rooted in the imperfection of electronic circuitry. Let us consider the usual tetrapolar electrode system illustrated in figure 6.

At port 1 a complex current i is introduced, and at port 2 the complex potential difference v is measured. From the CC electrodes the current spreads out in the tissue volume. The current density field in the tissue under the signal PU electrodes determines the measured potential difference.

Corresponding black box models are shown in figure 7. We study the signal transfer from port 1 to port 2, in this case

by the parameter complex transfer impedance Z_{tr} defined as

$$Z_{tr} = v/i.$$

Figure 7(a) is realistic if both the current source and the potential measuring circuits are ideally floating with respect to a common reference or ground potential. However, even modern electronic circuitry usually has some reference to ground and the voltage amplifiers have three terminal inputs in order to cancel CMS. Figure 7(b) shows a more realistic circuit example with the low end of the current carrying (CC) lead grounded. We will use this example to illustrate the problems more in detail.

Figure 8 shows simplified equivalent circuits for the tissue shown in figure 6 and for the potential measuring electronics. The tissue box has two complex impedances $Z1$ and $Z2$ related to the CC electrodes and their proximal volumes. $Z3$ represents the bulk volume and $Z4$ – $Z6$ the impedances related to the current density field under the PU electrodes. The circuit box shows usual two buffer operational amplifiers (gain +1), an inverting amplifier (gain –1) and an amplifier summing the non-inverted and inverted signals. The input CMV range is limited by the power supply voltage V_s for the operational amplifiers. The differential amplifier must therefore be referenced to the tissue to limit the CMV. Instead of using five electrodes, the reference lead of the amplifier and the low end of the current source are connected using a common electrode.

If the resistor balance is ideally trimmed, the CMS is completely cancelled resulting in zero error voltage contribution. If imperfectly trimmed, the CMS contributes with an error signal in v_m . The phase of the CM error signal is toggled 180° each time the balance trimming point is passed. An imperfect differential amplifier will therefore either add or subtract its contribution to v_m . The CMS of v will depend on $Z1$ and $Z2$.

As an example, figure 9 shows measurement results obtained with a Solartron 1260 + 1294 impedance analyzer system with 100 mV rms excitation voltage. Impedance was first measured with the CC1 and PU1 leads connected to one side of a 1 kΩ resistor and the CC2 and PU2 leads to the other side of the resistor. The measured voltage was therefore 100 mV rms, the measured current 100 μA. Then the PU electrodes were coupled together and coupled first to the CC1 side of the resistor. Both the CMV and differential voltage was then zero. An ideal instrumentation should give 0 Ω but the result was about 0.007 Ω equivalent to a differential voltage of 0.7 μV at LF and 80 μV at HF. Then the two PU leads were coupled to the C2 side for max CMV (100 mV rms). The equivalent differential voltage increased to about 30 μV at LF and 1.8 mV at HF. With low CMV the phase angle toggled between + and –180° due to noise. With high CMV the phase of the error voltage increased to +96° at HF.

The results show that considerable error signals are introduced by CMV signals in ordinary electronic designs and that the errors increase with frequency. Due to the critical balance condition in the CMS rejection circuits the resultant error voltage and therefore also the transfer parameters may be unpredictable. It is important to reduce the CMV, and a third electrode supplying a tissue reference voltage for the amplifier

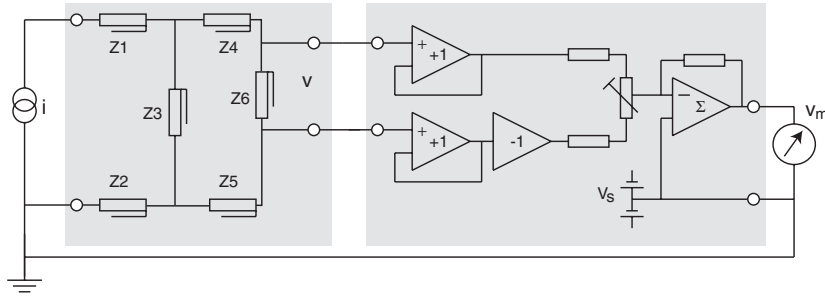


Figure 8. Equivalent circuits for tissue and a potential amplifier. The impedance symbol is for frequency dependent components.

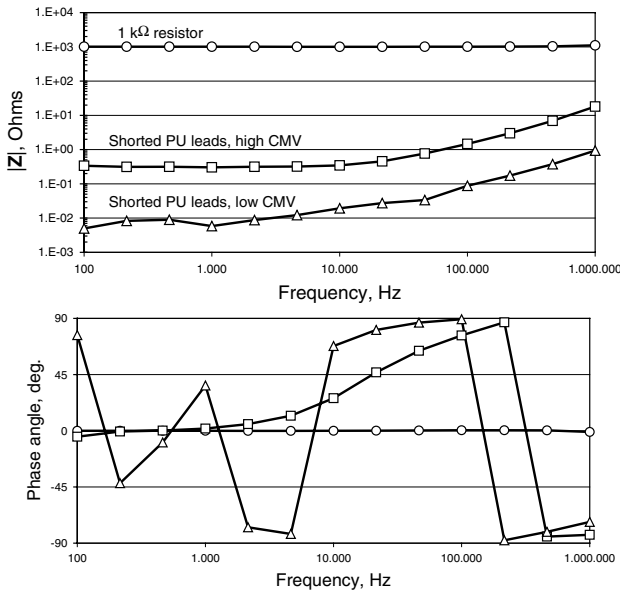


Figure 9. CMV influence with a Solartron 1260 + 1294 system measuring on a 1 kΩ resistor.

is necessary. As we have seen this does not necessarily lead to a five electrode system. In figure 8 small CMV are obtained by keeping $Z1 \gg Z2$, e.g. by using a large electrode for the CC1 lead.

The CMV problem is related to technology, and in the future small battery operated current sources and potential measuring units with telemetry may reduce or solve the CMV problems.

5. Surface shunt paths

A special case of the problems generated by different current paths is that of well conducting surface layers. This may be the case, for example, when measuring with surface electrodes on very moist skin or when using an array of surface electrodes where some of the current goes through the metal of passive electrodes placed between the CC electrodes. The most common result of such geometries is that the potential of the PU electrodes is brought to a level which is closer to that of the CC electrodes, leading to an overestimation of the transfer impedance. Measured positive phase angle can also be the result and there is a need for more research to investigate the possible consequences of this very common condition.

6. Inductive properties

Positive phase characteristics may be interpreted as if the material possesses inductive properties. Even if inductive properties have been reported also in biomaterials, in particular in the cell membrane studies [14, p 77], it is not likely to be found under stable conditions in passive bioimpedance measurements on macro tissue samples. However, positive phase angle is not necessarily a sign of measurement error. When measuring at high frequencies on set-ups giving low transfer impedance, self-inductance may give a considerable contribution.

The self-inductance of a wire is of the order of $1 \mu\text{H m}^{-1}$, dependent on the loop size/geometry and the thickness of the wire (higher values with thinner wire). The inductive reactance (ωL) amounts to 6.3Ω for $L = 1 \mu\text{H}$ at 1 MHz ($\omega = 2\pi 10^6$). Clearly the inductance cannot be neglected when measuring low impedance values (e.g. $< 50 \Omega$) at higher frequencies (e.g. $> 200 \text{ kHz}$). With two- and three-electrode measuring systems the measuring lead inductance is in series with the tissue impedance and therefore included in the results. With four-electrode systems the inductance should be limited to that of the measured tissue segment ($< 1 \mu\text{H}$); however, instrumentation errors may add to these figures in the form of poor common-mode rejection ratios at higher frequencies.

The self-inductance of the tissue may be regarded as a ‘true’ inductive property. As for the leads it is related to the geometrical dimensions, in particular the length. In addition it will be dependent on the total current loop of which it is a part.

With the self-inductance in series with the high frequency tissue resistance R the impedance is

$$Z = j\omega L + R.$$

It is clear that the inductive influence will be larger the lower the value of R . This may be an explanation why positive phase characteristics are seldom seen at 1 MHz for values of $R > 100 \Omega$, as illustrated in figures 10 and 11.

7. Error control

Sensitivity field calculations are very useful for avoiding some of the error sources mentioned in this paper. They provide an indispensable tool for optimizing electrode configuration and geometry in order to focus the measurements on the desired volume of the material. They can moreover be used for

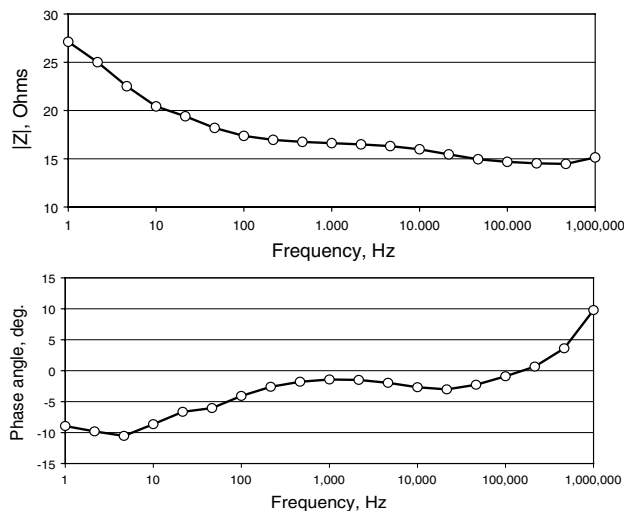


Figure 10. Four underarm skin surface electrodes with 4 cm centre separation. Each electrode 3 cm³ gel wetted area.

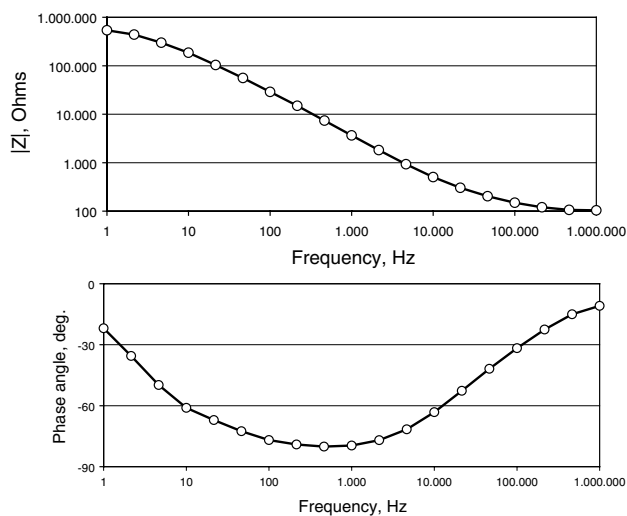


Figure 11. Three underarm skin surface electrodes with 4 cm centre separation. Same electrodes and site as for figure 10.

analysing the effect of conducting surface layers when, for example, using surface electrodes on human skin. The possible influence from conducting surface layers can also be studied by comparing measurements done first after applying a thin layer of moisture on top of the skin and then after wiping the skin dry with a paper towel.

Some of the other error sources mentioned in this paper can be detected by using one or more of several possible techniques. The reciprocity theorem states that interchanging the CC electrodes with the voltage PU electrodes should produce the same measuring result. This is valid under linear conditions, so if, for example, the voltage PU electrodes are very small the system can become non-linear when suddenly driving a large current through them, and reciprocity does no longer apply.

Another example of techniques that can be utilized for error control is the Kramers–Kronig transform [15]. This

transform gives the relationship between, for example, the real and imaginary parts of the immittance if the linear network function of frequency for one of them is known over the complete frequency spectrum. Hence, one can measure the resistance over a certain frequency range, make a regression to fit the data to a known function and then calculate the reactance. Or, one can calculate the phase angle from the impedance modulus. Apart from the obvious benefit of reducing instrumentation complexity in some applications, this technique also represents a useful check for experimental data consistency when both components of the impedance are measured.

8. Conclusions

The tetrapolar electrode system is commonly used because of its declared ability to eliminate the contribution from electrode polarization impedance in the measured data. However, tetrapolar measurements are more vulnerable to errors than monopolar or bipolar measurements. Some possible error sources have been described in this paper, but more research is needed before the behaviour of tetrapolar electrode systems on complex materials such as biological tissue can be fully understood.

References

- [1] Plonsey R and Barr R C 1988 *Bioelectricity. A Quantitative Approach* (New York: Plenum)
- [2] Miller H A and Harrison D C 1974 *Biomedical Electrode Technology. Theory and Practice* (New York: Academic)
- [3] Grimnes S and Martinsen Ø G 2002 Positive phase transfer impedance with the 4-electrode method *IFMBE Proc.* **2** 210–11
- [4] Grimnes S and Martinsen Ø G 2003 Positive phase bioimpedance and system inductive properties *IFMBE Proc.* **4** 2003
- [5] Schwan H P 1963 *Physical Techniques in Biological Research* vol 6, ed W L Nastuk (New York: Academic) pp 323–429
- [6] Geddes L A and Baker L E 1989 *Applied Biomedical Instrumentation* (New York: Wiley Interscience)
- [7] Brown B H, Wilson A J and Bertemes-Filho P 2000 Bipolar and tetrapolar transfer impedance measurements from volume conductor *Electr. Lett.* **36** 2060–2
- [8] Kramers H A 1926 Theory of dispersion in the X-ray region *Phys. Z.* **30** 52
- [9] Kronig R de L 1929 The theory of dispersion of X-rays *J. Opt. Soc. Am.* **12** 547
- [10] Geselowitz D B 1971 *IEEE Trans. Biomed. Eng.* **18** 38–41
- [11] Kuo F F 1966 *Network Analysis and Synthesis* (New York: Wiley)
- [12] Gersing E, Schafer H and Osypka M 1995 The appearance of positive phase angles in impedance measurements on extended biological objects *Innov. Tech. Biol. Med.* **16** 71–6
- [13] Grimnes S and Martinsen Ø G 2000 *Bioimpedance and Bioelectricity Basics* (San Diego, CA: Academic)
- [14] Cole K S 1972 *Membranes, Ions and Pulses* (Berkeley, CA: University of California Press)
- [15] Riu P J and Lapaz C 1999 *Electrical Bioimpedance Methods: Applications to Medicine and Biotechnology* ed P J Riu (New York: New York Academy of Sciences) pp 374–80